Distinct T cell receptor signaling pathways drive proliferation and cytokine production in T cells

Clifford S. Guy[1], **Kate M. Vignali**[1], **Jamshid Temirov**[2], **Matthew Bettini**[1], **Abigail E. Overacre**[1], **Matthew Smeltzer**[3], **Hui Zhang**[3], **Johannes B. Huppa**[4], **Yu-Hwai Tsai**[5], **Camille Lobry**[6], **Jianming Xie**[7], **Peter J. Dempsey**[5], **Howard C. Crawford**[8], **Iannis Aifantis**[6], **Mark M. Davis**[7], and **Dario A.A. Vignali**[1]

[1]Department of Immunology, St. Jude Children's Research Hospital, Memphis, TN, USA

[2]Cell and Tissue Imaging Shared Resource, St. Jude Children's Research Hospital, Memphis, TN, USA

[3]Department of Biostatistics, St. Jude Children's Research Hospital, Memphis, TN, USA

[4]Center for Pathophysiology, Infectiology and Immunology Institute for Hygiene and Applied Immunology, Immune recognition Unit, Medical University of Vienna, Austria

[5]Department of Pediatrics and Communicable Diseases, University of Michigan, Ann Arbor, MI, USA

[6]Howard Hughes Medical Institute, and Department of Pathology and NYU Cancer Institute, New York University School of Medicine, New York, NY, USA

[7]Howard Hughes Medical Institute, and Department of Microbiology and Immunology, Stanford School of Medicine, Palo Alto, CA, USA

[8]Mayo Clinic Cancer Center, Department of Cancer Biology, Jacksonville, FL, USA

Summary

The physiological basis and mechanistic requirement for the high immunoreceptor tyrosine activation motifs (ITAM) multiplicity of the T cell receptor (TCR)-CD3 complex remains obscure. Here we show that while low TCR-CD3 ITAM multiplicity is sufficient to engage canonical TCR-induced signaling events that lead to cytokine secretion, high TCR-CD3 ITAM multiplicity is required for TCR-driven proliferation. This is dependent on compact immunological synapse formation, interaction of the adaptor Vav1 with phosphorylated CD3 ITAMs to mediate Notch1 recruitment and activation and ultimately c-Myc-induced proliferation. Analogous mechanistic

events are also required to drive proliferation in response to weak peptide agonists. Thus, the TCR-driven pathways that initiate cytokine secretion and proliferation are separable and co-ordinated by the multiplicity of phosphorylated TCR-CD3 ITAMs.

T cells are a fundamental component of the adaptive immune system. Ligation of the T cell receptor (TCR) with antigenic peptide bound to major histocompatibility complex (MHC) molecules on antigen presenting cells (APCs) initiates a diverse array of developmental and functional events. These include T cell selection, differentiation, proliferation and cytokine production, which are optimally tailored to provide an appropriate response to the broad array of infectious agents that the host might encounter. The TCR is one of the most complex receptors in the immune system, consisting of the TCRα-TCRβ dimer plus three CD3 subunit dimers CD3ε-CD3γ, CD3ε-CD3δ and CD3ζ-CD3ζ which assemble in a coordinated manner[1]. Although many immune system receptors are multi-chain complexes, the necessity for such receptor complexity remains elusive. However, it is possible that this complexity is an essential requirement for their ability to mediate multiple downstream events.

Intracellular signaling is initiated upon phosphorylation of immunoreceptor tyrosine activation motifs (ITAMs) contained within the CD3 cytoplasmic domains. Although utilization of ITAMs is widespread among receptors expressed by other cell types of the immune system, including B, NK or myeloid cells, this is usually restricted to the inclusion of just one or two motifs (low ITAM multiplicity). In contrast, the TCR-CD3 complex contains 10 (high ITAM multiplicity) even though many of the same signaling molecules and pathways are initiated as more simplistic receptors. The physiological and mechanistic basis for this complexity and high ITAM multiplicity remains to be fully understood.

Tyrosine phosphorylation of the ITAMs by the Src-family kinases Lck, which is predominantly associated with the CD4 or CD8 co-receptors, and Fyn, leads to the recruitment of the kinase ZAP-70 via its tandem SH2 domains[2]. Subsequent ZAP-70 activation facilitates phosphorylation of the scaffolding proteins LAT and SLP-76[3] which provides a multitude of SH2 and SH3 binding sites for the propagation of downstream signaling events, including cytoskeletal rearrangement via the adaptor molecule Vav1, activation of distal canonical signaling pathways via ERK or nuclear localization of key transcription factors such as NFAT[4]. Many of these events are critical for cytokine induction, but the signaling pathway required to induce T cell proliferation remains obscure.

Antigen recognition leads to a redistribution of TCR-CD3 complexes along with co-stimulatory and adhesion proteins into a defined immunological synapse (IS) necessary for productive T cell activation[5, 6]. Early reports showed an enrichment of TCR, CD28 and Lck molecules within a defined central supramolecular cluster (cSMAC), surrounded by the adhesion molecule LFA-1 and its binding partner ICAM-1 in the peripheral supramolecular cluster (pSMAC), which is itself circumscribed by an area rich in regulatory molecules including CD45, termed the distal supramolecular cluster (dSMAC)[7]. Subsequent demonstrations of the importance of TCR microclusters for the initiation of signaling challenged the initial view that the mature IS was required for sustained TCR-induced signaling, and suggested instead that continued signaling in the periphery of the IS was

followed by termination of TCR signals and regulation of the response within the well-defined cSMAC[8, 9]. It is well understood that phosphorylation of early TCR signaling proteins, recruitment of key adaptor proteins and initiation of calcium flux occurs within the peripheral microclusters, which are subsequently transported into the cSMAC as a result of cytoskeletal rearrangements driven in part by Vav[8].

We recently generated mice expressing TCR-CD3 complexes with different numbers of non-functional mutant versus wild-type ITAM sequences[10–12]. Whereas a precisely linear relationship between the number of functional ITAMs and the proliferative capacity of the responding T cell was observed, antigen-stimulated cells retained the capacity to secrete cytokines such as interleukin 2 (IL-2) and interferon-γ (IFN-γ). In this study we examined which aspects of IS formation and proximal signaling events underlie the uncoupling of proliferative and cytokine responses. Specifically, we addressed whether T cells with low ITAM multiplicity (ie. only possessing 2–4 intact, functional ITAMs) retained their capacity to initiate TCR proximal signaling events including phosphorylation of key signaling molecules, to mobilize the cytoskeleton leading to formation the of a mature IS, to activate classical downstream targets of TCR ligation and to engage pathways that are not immediate targets of TCR-associated kinases but are essential for T cell proliferation.

Methods Online

Mice

Rag1^{−/−} and C57BL/6J mice were from Jackson laboratories (Bar Harbor, ME). *Adam10*^{fl/fl} mice were provided by PJ Dempsey (University of Michigan), while *Notch1*^{fl/fl} mice were provided by I Aifantis (NYU School of Medicine) and subsequently crossed to mice with Rosa26[CreERT2] mice. Generation of CD3εζ-KO (*Cd3e* [p/ p].*Cd247*^{−/−}) and CD3εζ-KO *Rag1*^{−/−} have been described[11]. All animal experiments were conducted according to institutional guidelines, in a Helicobacter- and MNV-free and specific pathogen-free facility accredited by the Association for the Assessment and Accreditation of Laboratory Animal Care. Animal protocols were by the Institutional Animal Care and Use Committee of St. Jude.

Cell sorting, intracellular staining and flow cytometric analyses

Spleens and lymph nodes were pooled from mice expressing WT or mutant CD3 ITAM sequences (5–10 mice per group) 5 weeks post reconstitution, prior to the onset of autoimmunity (Ref), and stained with fluorescently conjugated antibodies to discriminate naïve T cells on the basis of CD4^{+}CD25^{−}CD45RB^{high}. Sorted cells were additionally stained with fluorescently conjugated anti-TCRβ antibodies (H57-597; Biolegend, San Diego, CA) prior to flow cytometric analyses. For stimulation via CD3 crosslinking, sorted cells were labeled with anti-CD3ε antibodies (145-2C11; Biolegend) followed by goat anti-Hamster IgG to facilitate crosslinking. Cells were fixed and subsequently stained using antibodies directed against pZAP-70 or pERK (Cell Signaling Technologies, Danvers, MA) as previously described[45] prior to analysis by flow cytometry.

Retroviral-mediated stem cell gene transfer

Retroviral-mediated stem cell gene transfer using multicistronic vectors comprised of all four CD3 subunits linked via 2A peptides was performed as described[11]. For some experiments, Myc^{ERT2} was included (provided by D Green, St. Jude).

Lipid bilayers and microscopic analyses

Synthetic planar lipid bilayers containing anti-TCRβ antibodies and ICAM-1 adhesion molecules were constructed as previously described[46, 47]. For live cell imaging, sorted T cells were allowed to settle onto stimulatory lipid bilayers containing anti-TCRβ and ICAM-1 molecules. TCR microclusters were detected via fluorescently linked streptavidin which was coupled to the lipid bilayer and to biotinylated anti-TCRβ antibodies. Bilayers were imaged using a spinning disc laser scanning confocal system and TIRFM. Images were captured every 2 s using Slidebook acquisition and analysis software (3i technologies, Denver, CO), and the speed of microcluster movement as well as displacement was determined using a particle tracking algorithm following laplacian 2D filtering of raw images. FRET analyses were performed using TIRFM of lipid-bilayer stimulated T cells or transfected HEK293 cells, which were stained with antibodies specific for CD3ζ labeled with Alexa 546 (FRET donor) and Notch1 (ICD) or Vav1 antibodies labeled with Alexa647 (FRET acceptor). The corrected FRET image (FRETc) was generated by mathematical correction for donor bleed-through and direct excitation of acceptor using Slidebook software, and were further normalized based on the expression levels of the donor and acceptor.

Selected experiments utilized bilayers comprised of I-E^k molecules loaded with the AND TCR agonist peptide MCC labeled with Cy3, and the adhesion molecule ICAM-1 labeled with Cy5. Sorted cells derived from wild-type or CD3 ITAM mutant retrogenic mice were stimulated by exposure to the lipid bilayer for the times indicated, prior to fixation with 4% paraformaldehyde in PBS. Intracellular staining was performed following permeabilization with PBS containing 0.1% TritonX-100. Primary antibodies directed against pTy (4G10;Cell Signaling), Notch1 (MAB5414; Millipore, Billerica, MA) or ADAM10 (MAB946;R&D Systems, Minneapolis, MN), and in some cases fluorescently labeled phalloidin (Invitrogen, Carlsbad, CA), were added in PBS containing 1% FBS + 1% BSA and incubated overnight at 4 ° C. Following washing with PBS, fluorescently conjugated secondary antibodies were added for 1 h at RT, followed by washing and subsequent analysis using TIRFM. In selected experiments, cells were mixed with anti-CD3 and anti-CD28 coated beads (Invitrogen) at a 1:1 T cell to bead ratio. The mixture was centrifuged at 1200 rpm for 5 min to facilitate contact, with a subsequent incubation as indicated at 37 ° C. T cell-bead conjugates were fixed by addition of 4% paraformaldehye for 10 min, followed by washing and permeabilization with PBS containing 0.1% TritonX-100. Conjugates were stained with biotinylated anti-IL2 antibodies (Biolegend) in PBS containing 1% FBS + 1% BSA overnight at 4 ° C. Beads were subsequently detected with fluorescently conjugated goat anti-hamster IgG, whilst IL-2 was detected using fluorescently labeled streptavidin (Invitrogen). Fluorescently labeled phalloidin (Invitrogen) was utilized to detect the cellular cytoskeleton.

Plasmids and Cell Transfection

HEK293 cells (1×10^5) were transfected with MSCV-based 2A-peptide retroviral vectors encoding CD3 subunits and TCRαβ chains as described in the text and in detail elsewhere (Holst et al. 2008). Cells were additionally transfected with plasmids encoding human Vav1 upstream of an IRES and mCherry fluorescent reporter, and a constitutively active form of Lck wherein the regulatory Y505 has been mutated to phenylalanine (a gift from D. Littman) which was subcloned into a retroviral vector upstream of an IRES and YFP reporter. 72 h post transfection, cells were analyzed by flow cytometry for expression of the reporter plasmids. In addition, cells were prepared for Co-immunoprecipitation and Western blot analyses as described below. In parallel experiments, cells were plated on poly-L-lysine or αCD3-coated chambered coverslips for 3 h prior to fixation and analysis by TIRFM.

RNA, cDNA and quantitative real-time PCR

Gene expression following CD3 crosslinking was assessed by quantitative real-time PCR using the following primers and SYBR green detection: c-myc-F 5'-ttgaaggctggatttcctttgggc, c-myc-R 5'-tcgtcgcagatgaaatagggctgt; Hes1-F 5' aaagatagctcccggcattc, Hes1-R 5' tgcttcacagtcatttccaga.

Western blotting and immunoprecipitation

Western blot analyses of wild-type and CD3 ITAM mutant T blasts were performed following CD3 stimulation as outlined above. Cells were activated by CD3 crosslinking for the times indicated, followed by quick centrifugation and lysis in RIPA buffer containing protease and phosphatase inhibitors (Sigma, St.Louis, MO). 50μg of total protein was electrophoresed under denaturing conditions using a 4–12% bis-Tris gradient gel (Invitrogen). Proteins were transferred onto nitrocellulose membrane, blocked in 3% non-fat milk (BioRad, Hercules, CA), and probed with antibodies specific for Myc, Notch1 ICD (Cell Signaling) or actin (Sigma). Immunoprecipitation studies were performed using cells stimulated as above but which were lysed in buffer comprised of 20 mM Tris, 150 mM NaCl, 2 mM EGTA, 10% glycerol, 1% NP-40, and containing protease and phosphatase inhibitors as above. 100ug total protein was subjected to immunoprecipitation as previously described (Wang et al., 2010) using antibodies specific for Notch1 ICD or Nck1 (Cell Signaling) and protein G sepharose beads. Following washing, beads were subjected to denaturation, and eluted proteins were electrophoresed as above, followed by transfer to nitrocellulose and detection of co-immunoprecipitated proteins using anti-Vav1, anti-NotchICD, or anti-Nck1 antibodies (Cell Signaling).

Cre-mediated gene delivery and *in vitro* inhibition studies

Naïve CD4^{+} T cells were sorted from *Adam10*^{fl/fl} or from *Notch1*^{fl/fl} mice, and stimulated for 24 h using plate-bound anti-CD3 [1μg/ml] and soluble anti-CD28 [0.8μg/ml] antibodies. Cells were transduced with retrovirus containing a Cre-recombinase-IRES-mCherry construct, as previously described[48]. Following transduction (48 h), Cre+ and Cre– cells were sorted and restimulated *in vitro* with plate-bound anti-CD3 [0.01μg/ml] for 24 h prior to analysis of proliferation and cytokine expression. Gene deletion was confirmed in Cre+ cells by analysis of a fluorescent YFP reporter (*ADAM10*) or Western blot analyses

(*Notch1*). Naïve CD4^{+} T were sorted from WT C57BL/6J mice, and treated for 1 h on ice with the γ-secrestase inhibitor Z-LLNLe-CHO (Calbiochem, Darmstadt, Germany) prior to stimulation with plate-bound anti-CD3 [1μg/ml] and soluble anti-CD28 [0.8μg/ml] and analysis of proliferation and cytokine expression as noted in figure legend. Deletion of c-myc was performed by in vivo administration of tamoxifen (225mg/kg), and was confirmed by PCR analyses of the floxed Notch1 allele, Western blot and flow cytometric analyses.

Lentiviral-mediated gene delivery

Full length human Notch1 or a ligand-binding mutant lacking EGF repeats 11–12, were cloned into a third generation lentiviral vector (pCML20; courtesy of J Gray, SJCRH). Lentiviral particles were produced in HEK293T cells using calcium phosphate transfection, concentrated by ultracentrifugation, followed by determination of viral titre using standard techniques. T cells derived from tamoxifen-treated Notch1^{fl/fl}.Rosa[CreERT2] mice were activated for 24 h with plate-bound antiCD3 and antiCD28 followed by transduction with lentiviral particles at an MOI of 2:1. 48 h after transduction, cells were stained with a human-specific antiNotch1 antibody, followed by cell sorting and subsequent restimulation for 1 hr using planar lipid bilayers prior to analysis of c-myc induction by laser scanning confocal microscopy.

STORM

STORM analyses were performed using multicolor activator dye pairs as previously reported[29]. Images were acquired using Slidebook acquisition software, and TIRF illumination. Fluorescent fiduciary tetraspeck nanobeads were utilized to perform drift correction. STORM images were subsequently reconstructed using the QuickPALM Image J plugin, and composite images were displayed using Nikon Elements software.

Statistical analyses of STORM imaging data

Clustering was defined as a statistically significant departure from complete spatial randomness and evaluated using Ripley's K-function and L-function with 95% confidence envelopes. The proportion of clustering within a group was estimated based on the binomial distribution with exact 95% confidence intervals. Cluster analysis was performed in R Version 2.13.2.

Statistical analysis

Statistical significance of non-imaging data was determined with the unpaired Student's t-test or one way ANOVA, as appropriate. Prism GraphPad version 5.0 was used for statistical analyses.

Results

Low CD3 ITAM multiplicity preferentially affects proliferation

A linear relationship between the number of functional CD3 ITAM sequences (defined here as a wild-type, intact ITAM which can be phosphorylated and mediate downstream signaling, compared with mutant ITAMs [Tyr-Phe] which cannot) and the proliferative

capacity of naïve T cells following mitogenic or antigenic stimulation was previously demonstrated[11]. In depth analysis of isolated naïve CD4^{+} T cells derived from retrogenic mice expressing various combinations of wild-type and mutant CD3 ITAMs (CD3$\delta\gamma\varepsilon\zeta^{WT}$ – 10 ITAMs, CD3δ^{WT}CD3γ^{WT}CD3ε^{WT}CD3ζ^{WT} [referred to as CD3-10ITAM]; CD3$\delta\gamma\varepsilon^{WT}\zeta^{M}$ – 4 ITAMs, CD3δ^{WT}CD3γ^{WT}CD3ε^{WT}CD3ζ^{M} [referred to as CD3-4ITAM]; CD3$\varepsilon^{WT}\delta\gamma\zeta^{M}$ - 2 ITAMs, CD3δ^{M}CD3γ^{M}CD3ε^{WT}CD3ζ^{M} [referred to as CD3-2ITAM]; Fig. 1a) revealed that T cells expressing a full complement of wild-type CD3 subunits exhibited a dose-dependent proliferative response following TCR-CD3 ligation, while complexes containing a 4 or 2 functional ITAMs exhibited significantly impaired proliferative capacity (Supplementary Fig. 1a). Similar results were obtained using anti-CD3 and anti-CD28 coated beads (Supplementary Fig. 1b). Circumvention of TCR signaling via stimulation with phorbol 12-myristate 13-acetate (PMA) and ionomycin largely restored the proliferative capacity of CD3 ITAM mutant T cells (Supplementary Fig. 1c).

A full complement of wild-type CD3 subunits was not required for IL-2, IFN-γ or TNFα cytokine secretion in response to CD3 ligation (Supplementary Fig. 1d–f). Intracellular detection of IL-2 in response to anti-CD3/28 bead stimulation showed no overt defects in either expression or directed secretion of IL-2 (Supplementary Fig. 1g–i). Analyses of retrogenic T cells expressing all possible combinations of mutant CD3 subunits that possessed only 2 functional ITAMs showed that proliferative and cytokine responses following CD3 ligation were consistently uncoupled (Supplementary Fig. 1j,k).

High ITAM multiplicity is required to induce c-Myc expression

Given that T cells with low TCR-CD3 ITAM multiplicity exhibit a clear proliferative defect, we focused on pathways known to be required for the proliferation of multiple cell types. The c-Myc (*Myc*) proto-oncogene confers proliferative and survival signals in numerous neoplastic tissues, however c-Myc also plays essential roles in thymocyte development[13] and during the activation of mature T cells[14]. Expression of c-Myc is upregulated following TCR-CD3 ligation and stimulation with PMA and ionomycin[14]. We observed strong *Myc* mRNA and protein expression following TCR-CD3 ligation of CD3-10ITAM T cells, while c-Myc induction in CD3-2ITAM and CD3-4ITAM mutant T cells was deficient (Fig. 1b,c).

As expression of c-Myc is regulated by Notch-mediated signaling among other pathways, we analyzed the expression of *Hes1*, a key downstream indicator of Notch activation. We found a lack of *Hes1* induction in CD3-2ITAM and CD3-4ITAM T cells following TCR ligation (Fig. 1d). Activation of Notch1 and generation of the transcriptionally active Notch intracellular domain (NICD) fragment has been observed following TCR engagement[15, 16]. Immunoblot analysis showed a reduction in NICD generation following TCR stimulation of CD3-2ITAM and CD3-4ITAM blasts and naïve T cells as compared to CD3-10ITAM T cells (Fig. 1e, Supplementary Fig. 2a). CD3 ITAM mutant T cells also exhibited a defect in NICD nuclear translocation following TCR ligation (Fig. 1f).

We next addressed if expression of c-Myc could rescue the proliferative defect observed in CD3-2ITAM and CD3-4ITAM mutant T cells by expressing tamoxifen-regulated c-Myc (Myc[ERT2]). Adding tamoxifen *in vitro* induced the nuclear translocation of c-Myc (Fig. 1g) and completely rescued the proliferative defect of ITAM mutant T cells (Fig. 1h).

Notch signaling is required for T cell proliferation

We next asked whether inhibition of the Notch1 pathway in wild-type T cells could recapitulate the lack of cellular proliferation and maintenance of cytokine expression observed in low CD3 ITAM T cells. Multiple cleavage events yield the transcriptionally active NICD, including excision of the extracellular domain by the ADAM10 metalloprotease (Kuzbanian) and, to a lesser extent ADAM17 (TACE), followed by intracellular cleavage by the presenilin-containing γ-secretase complex[17]. Treatment of naïve T cells with a γ-secretase inhibitor (GSI) significantly reduced T cell proliferation, but did not affect cytokine production in response to CD3 cross-linking (Fig. 2a).

As pharmacological inhibition of the γ-secretase complex may have non-specific effects[18, 19], we assessed the contribution of the Notch pathway in driving T cell proliferation by genetic deletion of ADAM10 or Notch1. $Adam10^{fl/+}$ and $Adam10^{fl/fl}$ naïve CD4+ T cells were transduced with a retrovirus encoding Cre-recombinase and an IRES-linked fluorescent reporter. Transduced and non-transduced cells were sorted and restimulated for 24 h with plate-bound anti-CD3. Flow cytometric analysis confirmed retroviral Cre-mediated deletion of ADAM10 (Supplementary Fig. 2b). Although there was no inherent defect in the proliferative capacity of $Adam10^{fl/fl}$ versus $Adam10^{fl/+}$ T cells in the absence of Cre-recombinase expression, Cre-mediated deletion of ADAM10 significantly reduced the proliferative capacity of restimulated T cells, but had no effect on IL-2 secretion (Fig. 2b and data not shown). Similar results were obtained with $Notch1^{fl/fl}$ CD4+ T cells, confirming the requirement of Notch1 for optimal proliferation, but not IL-2 secretion (Fig. 2c and Supplementary Fig. 2c).

Initial experiments suggested that a 40–50% reduction in NICD resulted in greater than 95% reduction in c-Myc induction in TCR-stimulated CD3-4ITAM mutant T cells (Fig. 1c,e and Supplementary Fig. 2a). To assess this further, we titrated GSI to produce a graduated inhibition of Notch1 cleavage. Although a 50% reduction in NICD yielded an 80% decrease in c-Myc induction, this effect was only evident in a narrow window of GSI concentration (Supplementary Fig. 2d). As an alternative approach, tamoxifen treatment of heterozygote $Notch1^{fl/+}$ T cells expressing a Rosa^{CreERT2} allele induced a 14% reduction of NICD following T cell stimulation. c-Myc induction was only 4% lower in heterozygote $Notch1^{fl/+}$ T cells compared to $Notch1^{+/+}$ controls, and proliferative responses were largely unaffected in tamoxifen-treated $Notch1^{fl/+}$ T cells compared with the control (Supplementary Fig. 2e,f). These data suggest that Notch1 is largely haplosufficient in T cells, and that the manner of Notch1 activation governs the downstream induction of c-Myc and cell proliferation.

Finally we assessed whether Notch ligand binding was necessary for Notch-mediated induction of c-Myc. Tamoxifen-treated $Notch1^{fl/fl}$Rosa^{CreERT2} T cells were transduced with lentivirus encoding either wild-type human Notch1 (hNotch) or a mutant hNotch1 lacking EGF domains 11 and 12 (hNotch1-ΔEGF11-12) that is incapable of ligand binding[20]. Deletion of murine Notch1 was confirmed by flow cytometry (Supplementary Fig. 2g), and transduced cells were sorted using a human Notch1-specific antibody. Sorted cells were restimulated with surface-bound CD3 mAb, followed by microscopic determination of c-Myc induction (Fig. 2d,e). Cells transduced with wild-type hNotch1 expressed c-Myc at

levels comparable to control cells, while T cells expressing hNotch1- EGF11-12 induced less c-Myc. These data suggest that Notch1 activation in the context of TCR stimulation occurs as a consequence of ligand binding in *cis* on the responding cell as APCs were not present and single cell activation was observed limiting the possibility of interaction with another T cell in *trans*.

Low ITAM multiplicity initiates signaling for cytokine production

We next analyzed canonical signaling events initiated following TCR ligation to determine which pathways were maintained for productive cytokine secretion. CD3-2ITAM or CD3-4ITAMs facilitated ZAP-70 phosphorylation (Fig. 3a, Supplementary Fig. 3a) and ERK phosphorylation (Fig. 3b, Supplementary Fig. 3b) equivalent to wild-type TCR-CD3 complexes. Analysis of IS formation following stimulation with synthetic planar lipid bilayers containing lipid anchored anti-CD3ε and the adhesion molecule ICAM-1 revealed that CD3-10ITAM, CD3-2ITAM and CD3-4ITAM T cells form close contacts with the stimulatory surface (Fig. 3c). Comparable IS formation was initiated in wild-type and CD3 ITAM mutant cells, leading to the accumulation of TCR-CD3 microclusters and the recruitment of phosphotyrosine-containing proteins to the TCR contact area.

Distal TCR signaling events include the activation of several key transcription factors, such as NFAT[21]. The relocalization of NFAT from the cytosol to the nucleus is a reliable indicator of calcium signaling following TCR ligation. CD3-10ITAM, CD3-2ITAM and CD3-4ITAM mutant T cells activated NFAT in response to receptor ligation on a lipid bilayer (Fig. 3d). T cells with low CD3 ITAM multiplicity showed enhanced kinetics of NFAT nuclear translocation, because the proportion of nuclear NFAT was significantly increased following 15 minutes of stimulation (Fig. 3d). However, there was a progressive reduction of NFAT nuclear retention over time in CD3-2ITAM and CD3-4ITAM T cells, which did not occur in CD3-10ITAM T cells. High CD3 ITAM multiplicity is therefore not required to initiate activation of calcium-dependent, TCR-associated downstream signaling molecules. Down-regulation of TCR surface expression and up-regulation of the activation markers CD25 and CD69, remained largely intact in CD3-2ITAM and CD3-4ITAM T cells (Supplementary Fig. 4a–b). Thus, many canonical TCR-associated proximal and distal signaling events that are known to be required for cytokine production are intact in low CD3 ITAM multiplicity T cells.

IS maturation requires high ITAM multiplicity

Notch1 localization is regulated during IS formation between human CD4+ T cells and autologous DCs[22] or murine thymocytes[23]. We next tested if the macromolecular organization of the IS facilitates Notch1 activation, and if TCR-CD3 complexes with low ITAM multiplicity fail to orchestrate IS maturation. Initial IS assembly was intact in CD3-2ITAM and CD3-4ITAM T cells stimulated with anti-TCRβ-anchored lipid bilayers (Fig. 3c). Temporal analysis of IS formation showed that CD3-2ITAM and CD3-4ITAM T cells were able to form diffuse, immature IS, but were unable to undergo IS contraction, which is indicative of a mature, compact cSMAC, even after 60 min (Fig. 4a,b). This defect was consistently observed using T cells expressing TCR-CD3 complexes containing 2 functional ITAMs (Supplementary Fig. 4c,d).

Live cell imaging of naïve T cells following interaction with a stimulatory lipid bilayer (Supplementary Movies 1–3) revealed that although the number of microclusters formed and the speed of microcluster migration was similar between T cells expressing CD3-10ITAM, CD3-2ITAM or CD3-4ITAM complexes (Fig. 4c,d), the microclusters containing 2 or 4 functional CD3 ITAMs exhibited significantly reduced total (Fig. 4e) and endpoint (Fig. 4f) displacement. These data suggest that low CD3 ITAM complexes form microclusters and initially exhibit normal rates of mobility, but subsequently fail to form a compact cSMAC.

High ITAM multiplicity drives Notch1 recruitment to the cSMAC

Notch1 is known to accumulate within the cSMAC[22, 23]. Activation of Notch by ligand binding in *cis* or ligand-independent Notch activation have been described[15, 24, 25]. We investigated whether direct TCR-Notch interaction was required to facilitate Notch activation. Using AND TCR Tg T cells stimulated with a lipid bilayer containing pigeon cytochrome c peptide PCC_{81-103} bound to $H-2E^k$ and ICAM-1, we observed that the extracellular domain of Notch1, as well as ADAM10, became centralized within the mature cSMAC (Fig. 5a). APC-derived Notch ligands are not required for this redistribution.

In wild-type AND Tg T cells stimulated by lipid bilayers containing PCC_{81-103} pMHC and ICAM-1 Notch1 extracellular domain (Fig. 5b) and ADAM10 (Fig. 5c) co-localized with the TCR within the cSMAC. CD3-2ITAM and CD3-4ITAM AND Tg T cells did not form mature, compact cSMACs and showed diffuse ICAM-1 and TCR patterns (Fig. 5b,c), In these mutant cells, although Notch1 and ADAM10 co-localized with the TCR, as determined by Pearson's correlation coefficient, their distribution was also diffuse. The loose distribution observed may be insufficient to mediate Notch cleavage and activation, despite equivalent Notch1 surface expression (Supplementary Fig. 5a).

To determine if there was an intimate association between TCR and Notch in the IS, we used fluorescence resonance energy transfer (FRET) and TIRF microscopy, which can detect associations within 4–6nm. A high normalized FRET signal was observed between the intracellular domains of Notch1 and CD3ζ following TCR lipid-bilayer activation of CD3-10ITAM T cells. Less association was detected between Notch1 and CD3ζ in CD3-2ITAM and CD3-4ITAM T cells (Fig. 5d). Second, we utilized stochastic optical reconstruction microscopy (STORM)[26], which can detect associations within 30–50nm, to determine the occurrence of Notch1 in close approximation with TCR microclusters on wild-type and CD3 ITAM mutant T cells. Lipid bilayers containing antibodies against TCRβ induced TCR-CD3 complex clustering, which did not occur when T cells were tethered to the lipid bilayer via anti-CD44 (Supplementary Fig. 5b). We found a higher propensity for TCR microcluster-Notch1 co-occurrence in CD3-10ITAM compared with CD3-4ITAM and CD3-2ITAM T cells (Fig. 5e). Ripley's K cluster analyses of CD3 or Notch1 demonstrated that these molecules cluster and are not randomly distributed on the cell surface, in response to TCR lipid-bilayer stimulation. (Supplementary Fig. 5c). The tight linkage of these clusters, rather than their formation, was dysregulated in CD3-4ITAM and CD3-2ITAM T cells.

High ITAM multiplicity drives TCR-Vav1-Notch1 association

The initiation of TCR signaling occurs in peripheral microclusters, followed by transport towards the center of the cSMAC via a mechanism which is at least partially actin-dependent[8]. Vav1 is a guanine nucleotide exchange factor (GEF) for the Rho family GTPases that plays a pivotal role linking the TCR with cytoskeletal modifications[27, 28]. We tested whether defective TCR-Vav association was responsible for the incomplete maturation of the immune synapse in low CD3 ITAM cells. Immunoprecipitation assays revealed low constitutive Vav1 association with TCR-CD3 in resting CD3-10ITAM and CD3-2ITAM mutant T cell blasts. Following CD3 ligation there was a modest but significant increase in Vav1 recruitment to the TCR in CD3-10ITAM but not CD3-2ITAM mutant T cells (Fig. 6a,b). FRET analyses showed a close association between the CD3ζ chain and Vav1 in CD3-10ITAM T cells stimulated with anti-TCRβ embedded in planar lipid bilayers (Fig. 6c) while the CD3-Vav1 association was significantly lower in CD3-4ITAM and CD3-2ITAM T cells.

To control for the possibility that the association observed in immunoprecipitation and FRET experiments was mediated via another adaptor or by independent association with the LAT signalosome, we utilized a reductionist system to analyze the CD3-Vav association in the absence of known adaptor molecules[29]. Vav1 contains an SH2 domain that facilitates an interaction with LAT via the adaptor protein SLP-76 and also associates with phosphorylated ZAP-70[30]. Vav1 can also directly associate with an ITAM-like sequence in the cytoplasmic tail of the granulocyte receptor CEACAM3[31]. To test if Vav1 directly associates with phosphorylated ITAMs in the TCR-CD3 complex, HEK293 cells, which lack the adaptors Lck, ZAP-70, LAT and SLP-76 (Supplementary Fig. 6a) were transfected with Vav1, CD3-10ITAM, CD3-2ITAM or CD3-4ITAM mutant TCR:CD3 complexes, and a dominant-active Lck mutant to facilitate CD3 ITAM phosphorylation (Supplementary Fig. 6b). Immunoblot analyses demonstrated robust phosphorylation of the CD3-10ITAM CD3 complex, while CD3-4ITAM and CD3-2ITAM mutant complexes exhibited limited phosphorylation due to the reduced number of intact ITAMs (Supplementary Fig. 6c). FRET analyses in the transfected HEK293 cells showed a robust amount of FRET between Vav1 and CD3ζ in CD3-10ITAM TCR-CD3 complexes (Fig. 6d). Significantly less FRET was observed between Vav1 and CD3ζ in CD3-4ITAM and CD3-2ITAM mutant complexes. A basal level of FRET was similarly evident in all groups, probably due to protein overexpression (Supplementary Fig. 6d). However, only CD3-10ITAM CD3 complexes had increased association with Vav1 following transfection with dominantly active Lck (Supplementary Fig. 6d). These data suggest that Vav1 can directly associate with the TCR complex upon CD3 ITAM phosphorylation.

In co-immunoprecipitation analyses, the association between Notch1 with Vav1 was partially retained in CD3-4ITAM and CD3-2ITAM mutant T cells, while there was a dramatic reduction in the ability of TCR complexes to associate with Notch1 in mutant cells (Fig. 6e). We used multicolor activator STORM to analyze the distribution of the TCR-CD3 complex and Notch1 within the IS. A substantial number of TCR-CD3 microclusters exhibited close association with Vav and Notch1 in wild-type T cells (Fig. 6f). The adaptor protein Nck interacts with the CD3ε subunit[32] and facilitates Vav1 recruitment to the TCR

complex and subsequent mobilization of the actin cytoskeleton[33]. We examined whether Notch1 interacts with components of the actin regulatory network following CD3 complex ligation in T cells. Immunoprecipitation of Notch1 following TCR stimulation using anti-TCRβ antibodies showed increased association between Notch1 and Vav1, while Nck appeared to co-immunoprecipitate with Notch1 constitutively (Fig. 6b). STORM analyses of T cells lacking the PRS domain of the CD3ε chain (CD3ε- PRS) showed equivalent clustering of the TCR-CD3 complex or Notch1, as determined by Ripley's K analysis, and that the distribution of Notch1 within the IS was unperturbed in the absence of the CD3ε- PRS (Supplementary Fig 7a) suggesting that the CD3ε PRS motif was dispensable for Notch1 recruitment to TCR microclusters.

To test if the Vav1 SH2 domain mediated the interaction between Vav1 and the TCR complex, we used FRET to evaluate this interaction in the presence or absence of Zap70, which is known to exhibit high affinity for CD3 ITAMs. Overexpression of Zap70 displaced Vav1 from the TCR-CD3 complex (Fig. 6g). A single point mutation in the SH2-domain binding pocket of Vav1 (Vav1$^{R/K}$) blocked Vav1 association with the TCR complex, and this was independent of further Zap70 overexpression (Fig. 6g). Using two TCR-CD3 complex mutants in which all the first or all the second tyrosine residues in all the CD3 ITAM motifs were mutated to phenylalanine (designated 1-Y-F or 2-Y-F) showed that a single tyrosine within the ITAM motif resulted in an equivalent degree of FRET between Vav1 and CD3ζ, as observed for the CD3-10ITAM TCR complex. The FRET signal observed between Vav1 and the CD3ζ chain of 1-Y-F or 2-Y-F TCR-CD3 complexes was not disrupted by the addition of Zap70. These results suggest that a single tyrosine residue is sufficient to recruit Vav1 to the ITAM motifs, but insufficient to facilitate competition by Zap70 (Fig. 6g).

We next determined the kinetics of Zap70 or Vav1 association with the TCR complex. Co-immunoprecipitation analyses showed that both molecules followed similar rates of association with the TCR complex (data not shown). High resolution STORM analyses showed that 5 or 20 min stimulation of wild-type T cells using anti-TCR lipid bilayers resulted in the formation of TCR microclusters containing Zap70 or Vav1 (Fig. 6h and Supplementary Fig 7b), thus the occurrence of Zap70 or Vav1 within the TCR microclusters was not temporally or spatially regulated.

TCR affinity acts as a rheostat for T cell proliferation

To determine the physiologic basis for these observations, we interrogated whether weak peptide agonists induced low c-Myc expression and defective proliferation, as observed for low CD3 ITAM T cells. Stimulation of AND Tg T cells with control cognate peptide (PCC), super agonist (T102S) or weak agonists (K99A, K99E) showed increased proliferative responses to the super agonist, and diminished proliferation in response to weak agonists, compared with the control peptide (Fig. 7a)[34] However, AND Tg T cells secreted equivalent amounts of IL-2 in response to stimulation by APC pulsed with 10 μM control, super agonist, or weak agonist peptides (Fig. 7b).

c-Myc induction and nuclear translocation were enhanced in response to super agonist stimulation, and diminished following weak agonist stimulation, in comparison with the

control peptide (Fig 7c,d). Analyses of CD3-10ITAM, CD3-4ITAM or CD3-2ITAM mutant T cells expressing the AND Tg TCR and stimulated with PCC peptide-pulsed APC, showed that CD3-4ITAM and CD3-2ITAM mutants induced less c-Myc in response to antigenic stimulation (Fig. 7e,f).

Discussion

The importance and requirement for the large number of ITAMs within the TCR-CD3 complex for T cell development and functional activity remain elusive. Our data show that high CD3 ITAM multiplicity was necessary for IS maturation and T cell proliferation, but was dispensable to initiate canonical proximal and distal TCR signaling events and induction of certain cytokines. T cell proliferation required the recruitment of Vav1 to the CD3 complex for formation of a compact cSMAC, and aggregation of Notch1 along with the metalloprotease ADAM10 within the IS. A compact cSMAC is required for Notch activation, induction of c-Myc expression and proliferation.

Activation of the Notch signaling pathway leads to the induction of c-Myc and promotion of cellular proliferation[35]. The role of Notch activation in peripheral T cell responses remains controversial[36]. Whereas some studies suggest that Notch ligands control cell fate[15] and that Notch is necessary to promote cell cycle entry[37], others propose that Notch engagement significantly reduces T cell proliferative responses[38], Alternatively, some have suggested that Notch signaling plays no role in either T cell proliferative or lineage fate decisions and instead speculate it may serve to augment weak stimuli[16]. While our study suggest an important link between Notch and T cell proliferation, they do not infer that Notch signaling play no role in cytokine induction. Given this ambiguity, additional studies are clearly warranted.

Ubiquitination, endocytosis, receptor-ligand oligomerization, as well as mechano-transduction, contribute to Notch1 activation and signaling[39],[40]. Our experiments did not include recombinant or APC-presented Notch1 ligands, such as Jagged or Delta-like, even though Notch1 activation was observed. While we did not address this issue in detail, our data suggest that Notch activation may be *cis* ligand-dependent, as T cells expressing a non-ligand binding Notch mutant (hNotch1- EGF11-12) could not mediate c-Myc nuclear translocation. Furthermore, single T cells were imaged following stimulation of lipid bilayers or plate-bound anti-CD3 thereby limiting the possibility of ligation with another T cells in *trans*. However, additional experiments are clearly needed to determine how Notch is cleaved within the IS.

Our data demonstrate a clear reduction in Notch1 activation following ligation of low CD3 ITAM multiplicity TCRs. Consistant with an intimate TCR-Notch association, Notch1 has been shown to interact with p56[lck 41], and the E3 ligase and regulator of Notch activation, Numb, associates with components of the TCR signaling network including p56[lck], Vav and c-Cbl[23]. Here we showed that Notch1 interacts with Vav1 and the CD3 complex following TCR ligation. It is not clear whether Notch and the TCR are segregated in different protein islands which may concatenate following TCR stimulation, as has been previously reported

for the TCR and LAT[42]. Additional studies are needed to fully elucidate the TCR-Vav-Notch interaction.

Our demonstration that Notch1 associates with components of the TCR-associated cytoskeleton provides a mechanistic basis for the movement of Notch1 into the IS. Nck contains an SH2 domain and three additional SH3 domains that may facilitate linkage of the TCR with WAVE, WASP or other proteins involved in cytoskeletal mobilization[43]. Nck may interact directly with a proline rich sequence present in the cytoplasmic domain of Notch1 or may associate with additional proteins in a larger complex, possibly stabilized by the Notch1 ankyrin domains[44]. Furthermore, it might be predicted that destabilization of actin-dependent microcluster movement would result in defective Notch1 activation and abrogated induction of c-Myc[8].

Why is high ITAM multiplicity required for cytoskeletal remodeling and IS contraction? ZAP-70 contains two SH2 domains, and consequently has a superior capacity to associate with CD3 ITAMs than proteins containing a single SH2 domain[30]. While our data support this observation, we also showed that Vav1 can associate directly with the CD3 complex containing doubly or singly phosphorylated ITAM motifs. It remains possible that partial phosphorylation of CD3 ITAM motifs could recruit Vav1, while fully phosphorylated ITAMs readily bind Zap70. Our data indicate that Zap70 recruitment and activation does not require many intact ITAMs, thus high ITAM multiplicity may be required to increase the probability that Vav1 interacts with the CD3, thereby providing a link between the TCR and the cytoskeletal network.

In summary, our results suggest that high CD3 ITAM multiplicity presents the TCR with the unique capacity to mediate multiple modes of downstream signaling that drive distinct and separable functional events. The TCR-driven pathways that lead to cytokine production versus proliferation appear separable, which may allow the TCR-CD3 complex to promote limited effector function. A complete program of T cell differentiation and function may only occur following optimal TCR signaling, as suggested by our experiments using weak and strong peptide agonists. This may endow the TCR, and perhaps other multi-chain signaling receptor complexes, with the capacity to orchestrate a complex array of developmental and functional events and provide 'rheostat'-like control over the quality of the effector response.

Supplementary Material

Refer to Web version on PubMed Central for supplementary material.

Acknowledgements

References

1. Wucherpfennig KW, Gagnon E, Call MJ, Huseby ES, Call ME. Structural biology of the T-cell receptor: insights into receptor assembly, ligand recognition, and initiation of signaling. Cold Spring Harb. Perspect. Biol. 2010; 2 a005140.

2. Chan AC, Iwashima M, Turck CW, Weiss A. ZAP-70: a 70 kd protein-tyrosine kinase that associates with the TCR zeta chain. Cell. 1992; 71:649–662. [PubMed: 1423621]

3. Finco TS, Yablonski D, Lin J, Weiss A. The adapter proteins LAT and SLP-76 are required for T-cell activation. Cold Spring Harb. Symp. Quant. Biol. 1999; 64:265–274. [PubMed: 11232295]

4. Guy CS, Vignali DA. Organization of proximal signal initiation at the TCR:CD3 complex. Immunol. Rev. 2009; 232:7–21. [PubMed: 19909352]

5. Dustin ML, et al. A novel adaptor protein orchestrates receptor patterning and cytoskeletal polarity in T-cell contacts. Cell. 1998; 94:667–677. [PubMed: 9741631]

6. Monks CR, Freiberg BA, Kupfer H, Sciaky N, Kupfer A. Three-dimensional segregation of supramolecular activation clusters in T cells. Nature. 1998; 395:82–86. [PubMed: 9738502]

7. Fooksman DR, et al. Functional anatomy of T cell activation and synapse formation. Annu. Rev. Immunol. 2010; 28:79–105. [PubMed: 19968559]

8. Campi G, Varma R, Dustin ML. Actin and agonist MHC-peptide complex-dependent T cell receptor microclusters as scaffolds for signaling. J. Exp. Med. 2005; 202:1031–1036. [PubMed: 16216891]

9. Varma R, Campi G, Yokosuka T, Saito T, Dustin ML. T cell receptor-proximal signals are sustained in peripheral microclusters and terminated in the central supramolecular activation cluster. Immunity. 2006; 25:117–127. [PubMed: 16860761]

10. Holst J, Vignali KM, Burton AR, Vignali DA. Rapid analysis of T-cell selection in vivo using T cell-receptor retrogenic mice. Nat. Methods. 2006; 3:191–197. [PubMed: 16489336]

11. Holst J, et al. Scalable signaling mediated by T cell antigen receptor-CD3 ITAMs ensures effective negative selection and prevents autoimmunity. Nat. Immunol. 2008; 9:658–666. [PubMed: 18469818]

12. Szymczak AL, et al. Correction of multi-gene deficiency in vivo using a single 'self-cleaving' 2A peptide-based retroviral vector. Nat. Biotechnol. 2004; 22:589–594. [PubMed: 15064769]

13. Douglas NC, Jacobs H, Bothwell AL, Hayday AC. Defining the specific physiological requirements for c-Myc in T cell development. Nat. Immunol. 2001; 2:307–315. [PubMed: 11276201]

14. Lindsten T, June CH, Thompson CB. Multiple mechanisms regulate c-myc gene expression during normal T cell activation. EMBO J. 1988; 7:2787–2794. [PubMed: 3053165]

15. Amsen D, et al. Instruction of distinct CD4 T helper cell fates by different notch ligands on antigen-presenting cells. Cell. 2004; 117:515–526. [PubMed: 15137944]

16. Ong CT, Sedy JR, Murphy KM, Kopan R. Notch and presenilin regulate cellular expansion and cytokine secretion but cannot instruct Th1/Th2 fate acquisition. PLoS. One. 2008; 3:e2823. [PubMed: 18665263]

17. Selkoe D, Kopan R. Notch and Presenilin: regulated intramembrane proteolysis links development and degeneration. Annu. Rev. Neurosci. 2003; 26:565–597. [PubMed: 12730322]

18. Adler SH, et al. Notch signaling augments T cell responsiveness by enhancing CD25 expression. J. Immunol. 2003; 171:2896–2903. [PubMed: 12960312]

19. Minter LM, et al. Inhibitors of gamma-secretase block in vivo and in vitro T helper type 1 polarization by preventing Notch upregulation of Tbx21. Nat. Immunol. 2005; 6:680–688. [PubMed: 15991363]

20. Rebay I, et al. Specific EGF repeats of Notch mediate interactions with Delta and Serrate: implications for Notch as a multifunctional receptor. Cell. 1991; 67:687–699. [PubMed: 1657403]

21. Feske S. Calcium signalling in lymphocyte activation and disease. Nat. Rev. Immunol. 2007; 7:690–702. [PubMed: 17703229]

22. Luty WH, Rodeberg D, Parness J, Vyas YM. Antiparallel segregation of notch components in the immunological synapse directs reciprocal signaling in allogeneic Th:DC conjugates. J. Immunol. 2007; 179:819–829. [PubMed: 17617572]

23. Anderson AC, et al. The Notch regulator Numb links the Notch and TCR signaling pathways. J. Immunol. 2005; 174:890–897. [PubMed: 15634911]

24. Delwig A, Rand MD. Kuz and TACE can activate Notch independent of ligand. Cell Mol. Life Sci. 2008; 65:2232–2243. [PubMed: 18535782]

25. Hsieh EH, Lo DD. Jagged1 and Notch1 help edit M cell patterning in Peyer's patch follicle epithelium. Dev. Comp Immunol. 2012; 37:306–312. [PubMed: 22504165]

26. Bates M, Huang B, Dempsey GT, Zhuang X. Multicolor super-resolution imaging with photo-switchable fluorescent probes. Science. 2007; 317:1749–1753. [PubMed: 17702910]

27. Fischer KD, Tedford K, Penninger JM. Vav links antigen-receptor signaling to the actin cytoskeleton. Semin. Immunol. 1998; 10:317–327. [PubMed: 9695188]

28. Tybulewicz VL. Vav-family proteins in T-cell signalling. Curr. Opin. Immunol. 2005; 17:267–274. [PubMed: 15886116]

29. James JR, Vale RD. Biophysical mechanism of T-cell receptor triggering in a reconstituted system. Nature. 2012; 487:64–69. [PubMed: 22763440]

30. Wang H, et al. ZAP-Cold: an essential kinase in T-cell signaling. Spring Harb. Perspect. Biol. 2010; 2 a002279.

31. Schmitter T, et al. The granulocyte receptor carcinoembryonic antigen-related cell adhesion molecule 3 (CEACAM3) directly associates with Vav to promote phagocytosis of human pathogens. J. Immunol. 2007; 178:3797–3805. [PubMed: 17339478]

32. Gil D, Schamel WW, Montoya M, Sanchez-Madrid F, Alarcon B. Recruitment of Nck by CD3 epsilon reveals a ligand-induced conformational change essential for T cell receptor signaling and synapse formation. Cell. 2002; 109:901–912. [PubMed: 12110186]

33. Lettau M, et al. The adapter protein Nck: role of individual SH3 and SH2 binding modules for protein interactions in T lymphocytes. Protein Sci. 2010; 19:658–669. [PubMed: 20082308]

34. Rogers PR, Grey HM, Croft M. Modulation of naive CD4 T cell activation with altered peptide ligands: the nature of the peptide and presentation in the context of costimulation are critical for a sustained response. J. Immunol. 1998; 160:3698–3704. [PubMed: 9558070]

35. Radtke F, Fasnacht N, Macdonald HR. Notch signaling in the immune system. Immunity. 2010; 32:14–27. [PubMed: 20152168]

36. Yuan JS, Kousis PC, Suliman S, Visan I, Guidos CJ. Functions of notch signaling in the immune system: consensus and controversies. Annu. Rev. Immunol. 2010; 28:343–365. [PubMed: 20192807]

37. Joshi I, et al. Notch signaling mediates G1/S cell-cycle progression in T cells via cyclin D3 and its dependent kinases. Blood. 2009; 113:1689–1698. [PubMed: 19001083]

38. Eagar TN, et al. Notch 1 signaling regulates peripheral T cell activation. Immunity. 2004; 20:407–415. [PubMed: 15084270]

39. Bray SJ. Notch signalling: a simple pathway becomes complex. Nat. Rev. Mol. Cell Biol. 2006; 7:678–689. [PubMed: 16921404]

40. Kopan R, Ilagan MX. The canonical Notch signaling pathway: unfolding the activation mechanism. Cell. 2009; 137:216–233. [PubMed: 19379690]

41. Sade H, Krishna S, Sarin A. The anti-apoptotic effect of Notch-1 requires p56lck-dependent, Akt/PKB-mediated signaling in T cells. J. Biol. Chem. 2004; 279:2937–2944. [PubMed: 14583609]

42. Lillemeier BF, et al. TCR and Lat are expressed on separate protein islands on T cell membranes and concatenate during activation. Nat. Immunol. 2010; 11:90–96. [PubMed: 20010844]

43. Buday L, Wunderlich L, Tamas P. The Nck family of adapter proteins: regulators of actin cytoskeleton. Cell Signal. 2002; 14:723–731. [PubMed: 12034353]

44. Lubman OY, Korolev SV, Kopan R. Anchoring notch genetics and biochemistry; structural analysis of the ankyrin domain sheds light on existing data. Mol. Cell. 2004; 13:619–626. [PubMed: 15023333]
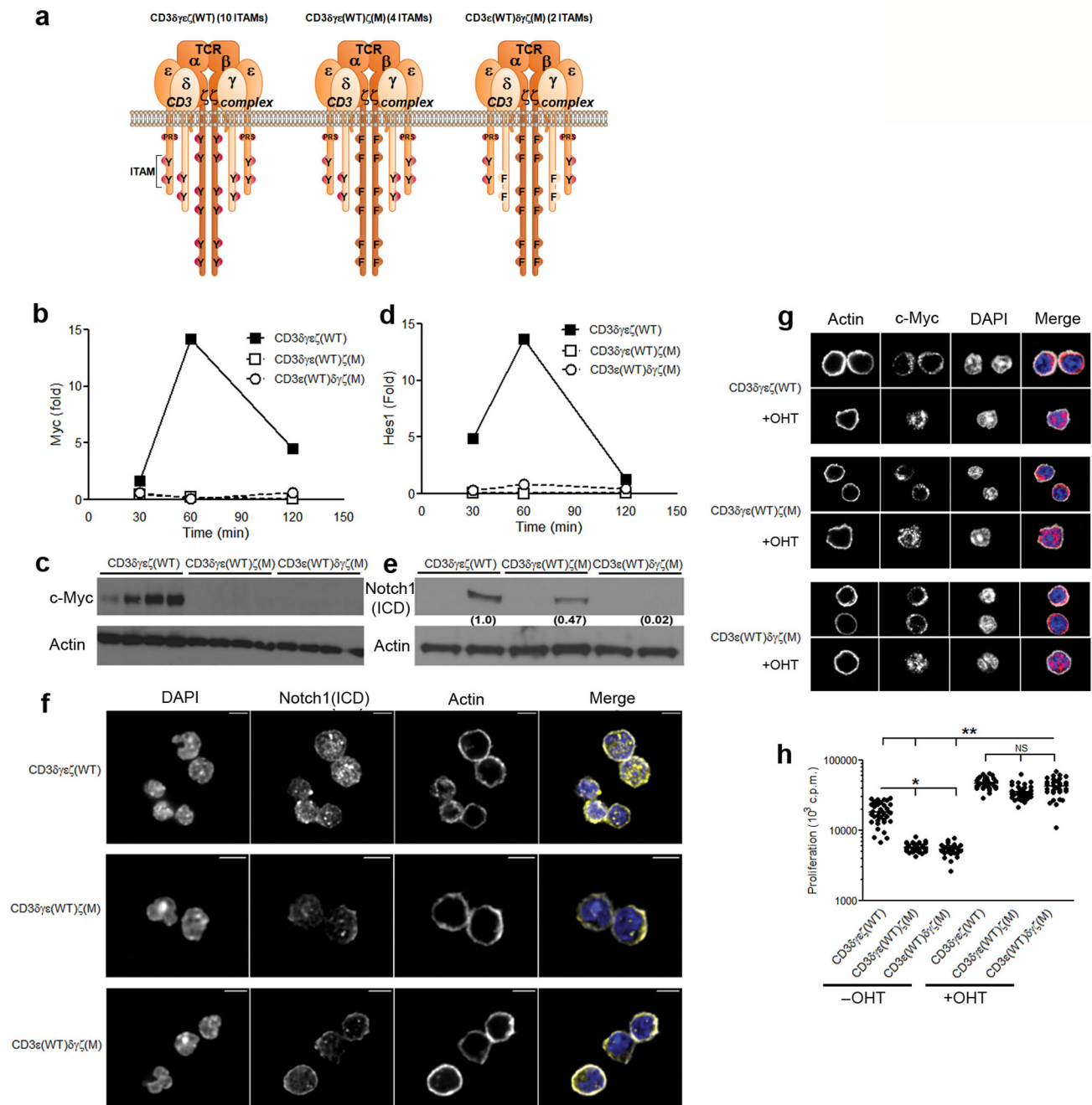
Figure 1. Ligation of low CD3 ITAM multiplicity complexes fails to induce c-Myc expression
(**a**) Schematic representation of the CD3 ITAM indicating the key tyrosine residues that were mutated to phenylalanine. (**b,c**) Expression of c-Myc mRNA assessed by quantitative PCR (**b**) o r immunobloting (**c**) in naïve CD4^{+} T cells stimulated for 24 h with PMA and ionomycin prior to culture with IL-2 for an additional 5 d. Cells were restimulated with anti-CD3 as indicated prior to analysis. (**d**) Quantitative PCR of *Hes1* mRNA expression in naïve CD4^{+} T cells treated as in **b**. (**e**) immunoblot analysis of Notch1 cleavage in naïve CD4^{+} T cells stimulated with plate-bound anti-CD3 and anti-CD28 antibodies as indicated prior to

lysis. Numbers in parentheses indicate relative intensity of NICD following normalization to actin. (**f**) Confocal microscopy of Notch1 ICD in resting CD4+ T cells blasts restimulated with anti-CD3 for 2 h prior to analysis. Merged image: DAPI (blue), Notch1 ICD (yellow) F-actin (grey). Data are representative of two independent experiments with 4–5 mice per group. (**g**) Confocal microscopy of of c-Myc localization in T cells expressing wild-type or mutant TCR:CD3 complexes and MycERT2 left untreated or stimulated for 24 h with tamoxifen. Representative images of 2 independent experiments are presented. Merged image: DAPI (blue), c-Myc (red) F-actin (grey). (**h**) Proliferation of wild-type or ITAM-mutant T cells expressing MycERT2 stimulated with anti-CD3 and anti-CD28 antibodies in the presence or absence of tamoxifen. Data are combined from 2 independent experiments with 10–15 mice per group. Scale bars represent 5μm. * p<0.005, ** p<0.0001
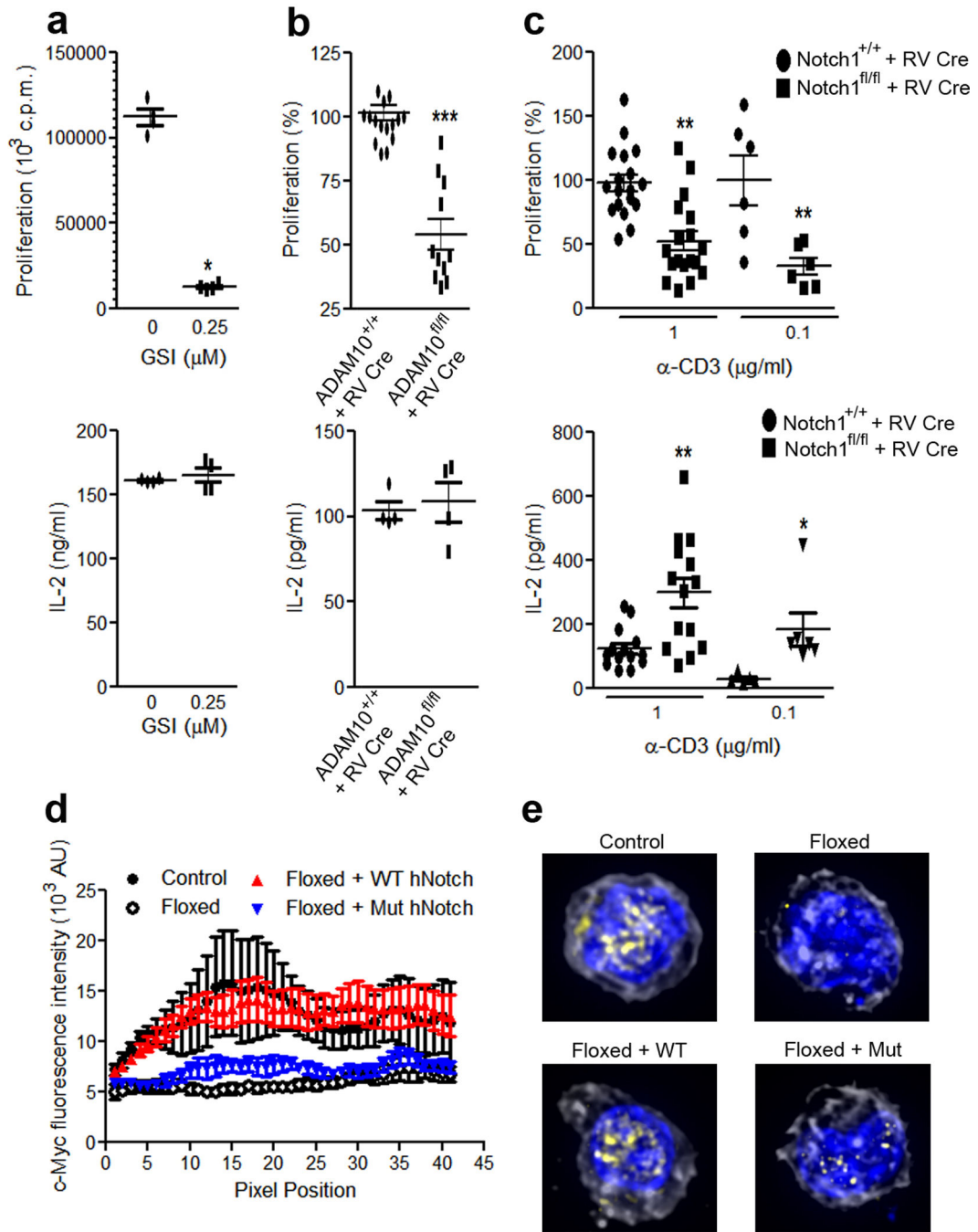
**Figure 2. Components of the Notch pathway are necessary for T cell proliferative but not cytokine responses**

(**a**) Proliferation (upper panel) and IL-2 secretion (lower panel) of naïve CD4^{+} T stimulated with anti-CD3 and anti-CD28 in the presence of a γ-secretase inhibitor. Data are representative of 4 independent experiments. (**b**) Proliferation (upper panel) and IL-2 secretion (lower panel) of CD4^{+} T cells from *Adam10*^{fl/fl} or Adam10^{+/+} mice transduced with RV Cre and restimulated with anti-CD3. (**c**) Similar experiments were performed using wild-type and *Notch1*^{fl/fl} T cells transduced with RV Cre. Data in (**b–c**) are representative of

2–3 independent experiments with at least 4 mice per group, and were determined to be significant where indicated using unpaired *t* tests or one way ANOVA as appropriate. (**d**) c-Myc induction was assessed in cells which expressed Notch1 (control), which were Notch1-null (floxed), or which expressed wild-type hNotch1 or mutant hNotch1- EGF11-12. Nuclear c-Myc is expressed as a line intensity, while representative images are presented in panel (**e**). Data are representative of three independent experiments. * p<0.02, ** p<0.001, *** p<0.0001.
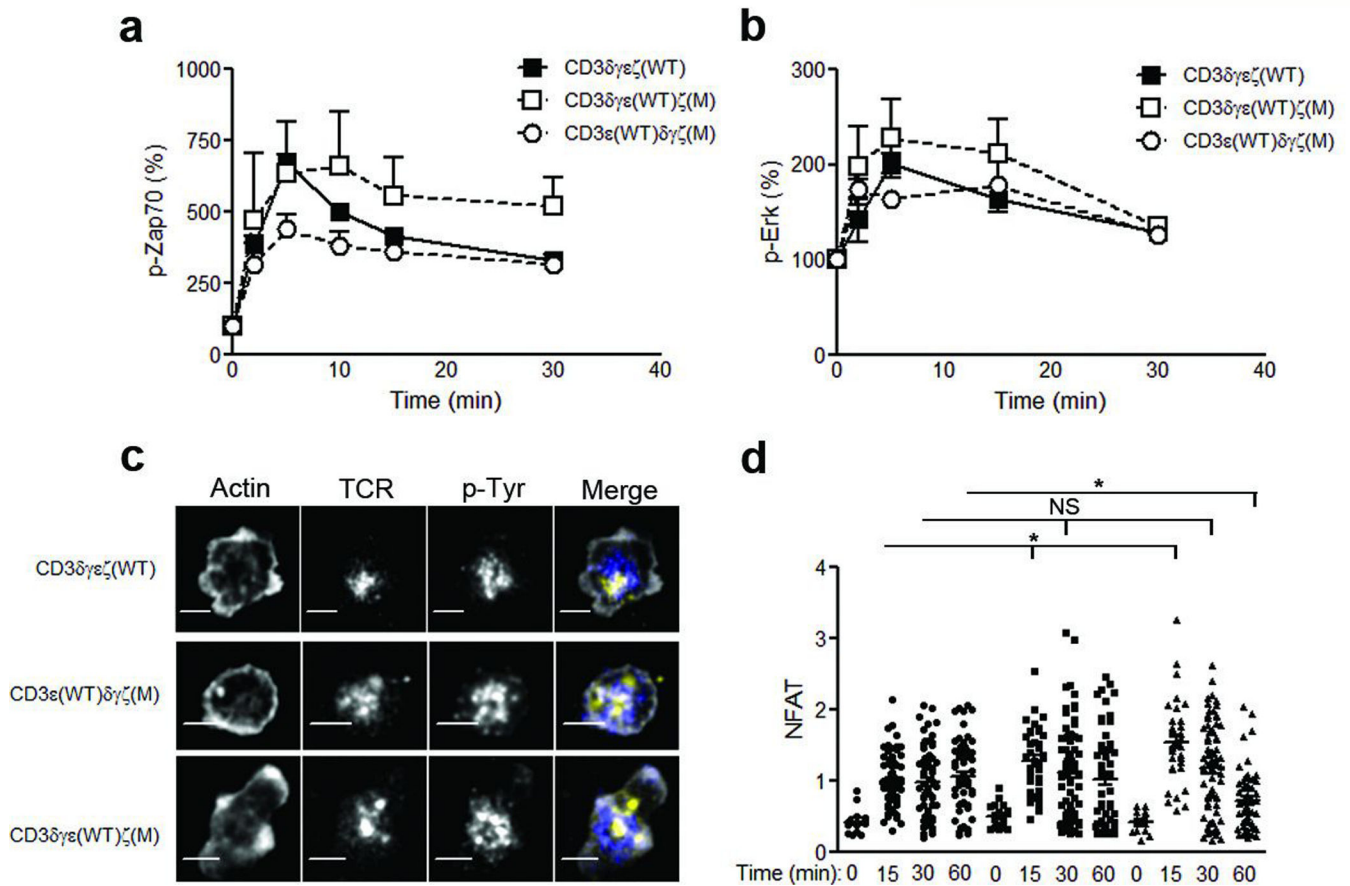
Figure 3. Initiation of canonical TCR signaling events following ligation of TCR:CD3 complexes with low ITAM multiplicity

(**a**) Analysis of pZap-70 or (**b**) p-ERK in TCR-stimulated Naïve CD4^{+} T. Mean fluorescent intensity values are presented relative to the Time 0 control designated as 100% (**c**) Microscopic analyses of TCR and p-Tyr distribution following stimulation of naïve CD4^{+} T cells with lipid bilayers containing anti-TCRβ antibodies. Images are representative of three independent experiments. (**d**) Nuclear:cytoplasmic ratiometric localization of NFAT was determined following stimulation of naïve CD4^{+} T cells with planar lipid bilayers. Graphical data represent the mean ± s.e.m. of three independent retrogenic experiments (n = 4–5 mice per group), while panel (**d**) depicts individual cells. Values were determined to be significantly different following one-way ANOVA testing. Scale bars represent 5μm. * $p < 0.05$.
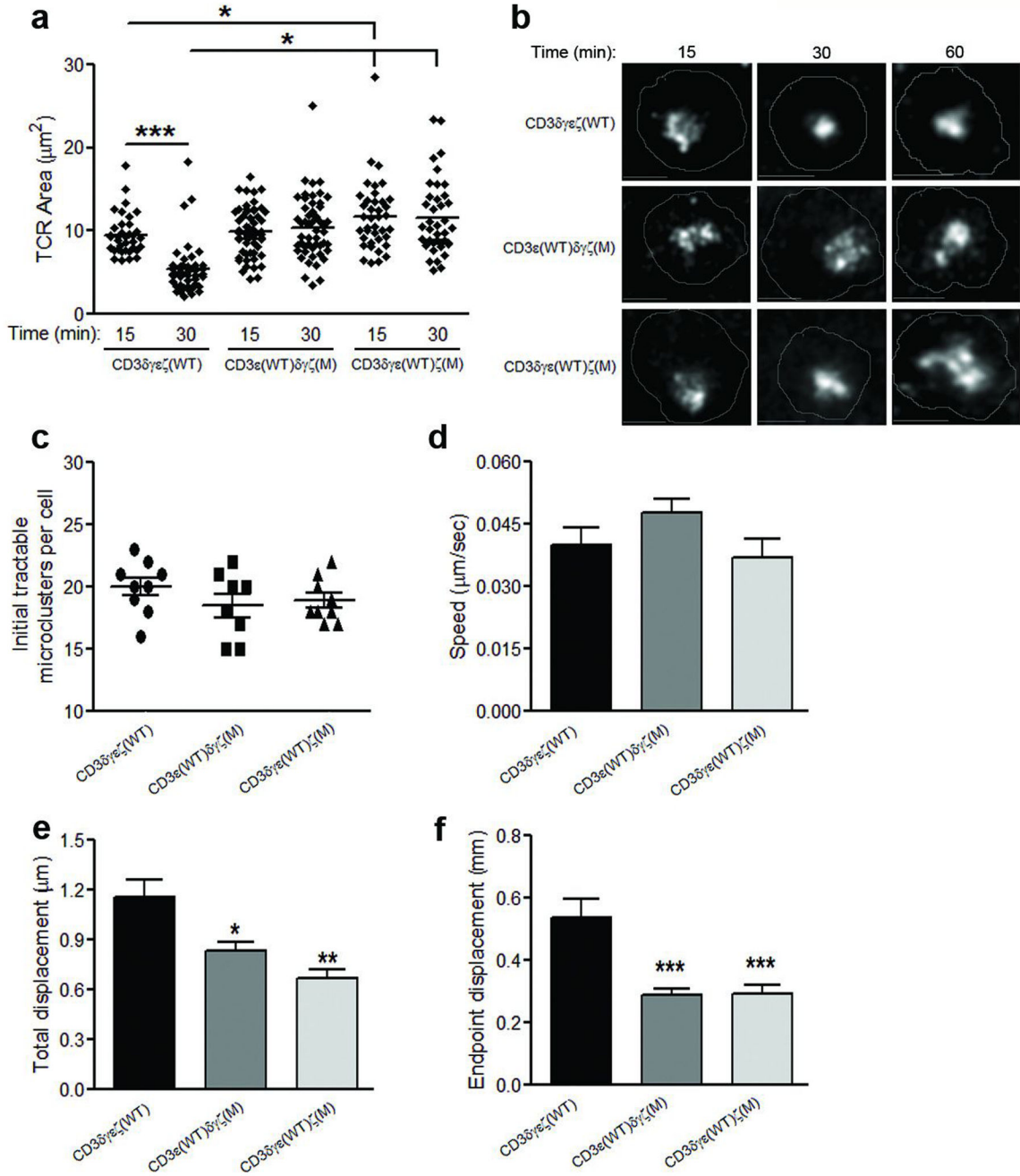
Figure 4. IS maturation requires high TCR:CD3 ITAM multiplicity

(**a**) Microscopic analyses of TCR distribution following stimulation of naïve CD4^{+} T with planar lipid bilayers containing anti-TCR antibodies. (**b**) Representative images of data depicted in (**a**). (**c–f**) Live imaging analyses of TCR microcluster particle formation (**c**), speed (**d**), total (**e**) and endpoint displacement (**f**) in response to stimulation with lipid bilayers as utilized in panels (**a**) and (**b**). Data are representative of two independent experiments (n = 4–5 mice per group), with significance determined as indicated using one-way ANOVA testing. Scale bars represent 5μm. * $p < 0.05$, ** $p < 0.01$, *** $p < 0.0001$.
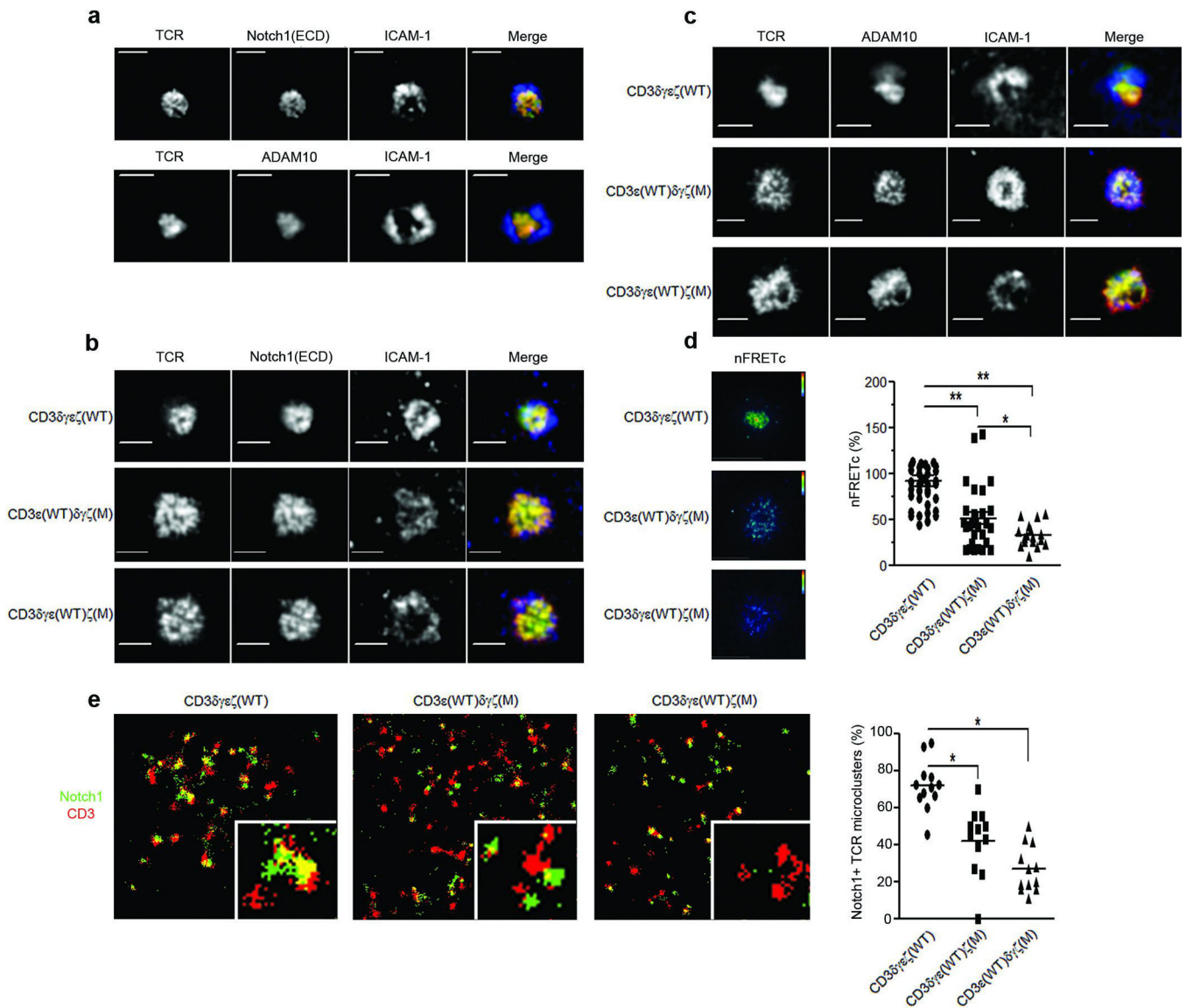
Figure 5. Components of the Notch1 activation pathway coincide with IS formation and exhibit diminished intermolecular interactions upon diminished ITAM multiplicity

(**a–c**) Analysis of Notch1 or ADAM10 distribution relative to TCR and ICAM-1 molecules following lipid bilayer stimulation of (a) wild-type AND TCR Tg CD4^{+} T cells or (**b,c**) wild-type or ITAM mutant AND TCR Tg retrogenic CD4^{+} T cells. Merged images in panels (**a–c**) depict TCR molecules in red, ICAM-1 molecules in blue, and Notch1 or ADAM10 molecules in green. Results are representative of two independent retrogenic experiments, with at least 15 cells analyzed per group. (**d**) Analysis of Notch1 and CD3ζ interactions in wild-type or ITAM mutant T cell blasts by FRET and TIRFM. (**e**) STORM analyses of Notch1 and CD3ζ distribution following lipid bilayer stimulation of wild-type or ITAM mutant T cells. Inset images depict enlarged microclusters. The proportion of TCR microclusters containing Notch1 is presented graphically. Representative images are shown, while graphical data are representative of 3 independent experiments with statistical

significance determined by one way ANOVA. Scale bars represent 5μm. Pixel size of STORM micrographs represent 30nm. *p<0.05, ** p<0.001.
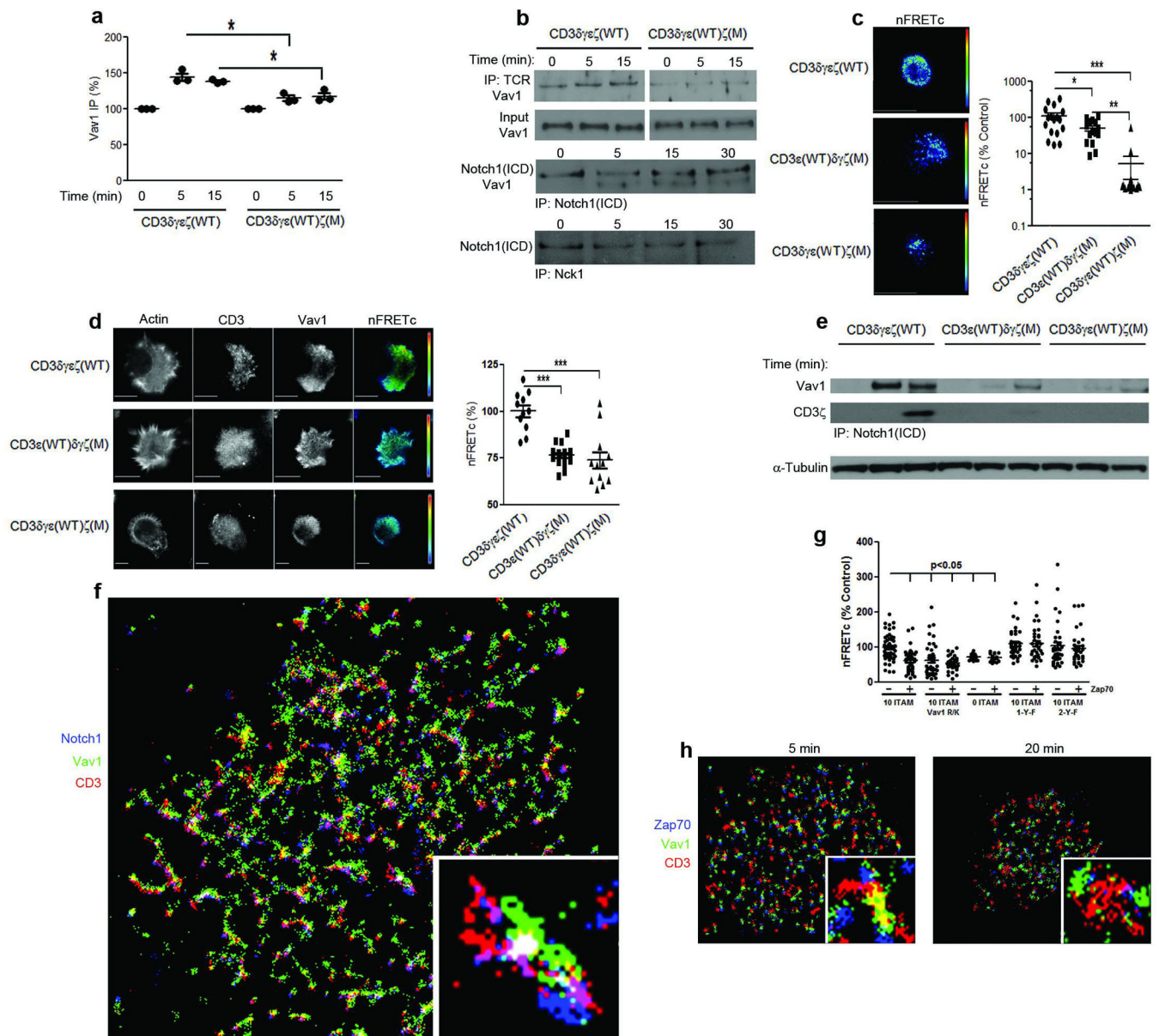
Figure 6. Low ITAM multiplicity results in diminished Vav1 recruitment to the CD3 complex
(**a,b**) Immunoprecipitation of the CD3 complex and analysis of Vav1 recruitment by Western blotting in wild-type or ITAM mutant CD4^{+} T cells. Data are presented relative to Time 0 control, designated as 100%, and are representative of three experiments. (**c**) TIRFM FRET analyses were performed on CD4^{+} T cell blasts using antibodies specific for Vav1 and CD3ζ, and are representative of two experiments. (**d** and **g**) TIRFM FRET analyses of Vav1 and CD3ζ interaction were performed using transfected HEK293 cells. (**e**) Co-immunoprecipitation analyses of wild-type or ITAM mutant CD4+ T cells following TCR ligation. Data are representative of two independent experiments, with 4–5 mice per group. (**f**) STORM analyses of Notch1, Vav1 and CD3ζ following lipid bilayer stimulation of wild-type CD4+ T cell blasts. (**h**) STORM analyses of Zap70, Vav1 and CD3ζ were conducted following lipid bilayer stimulation of wild-type CD4+ T cells. STORM data are
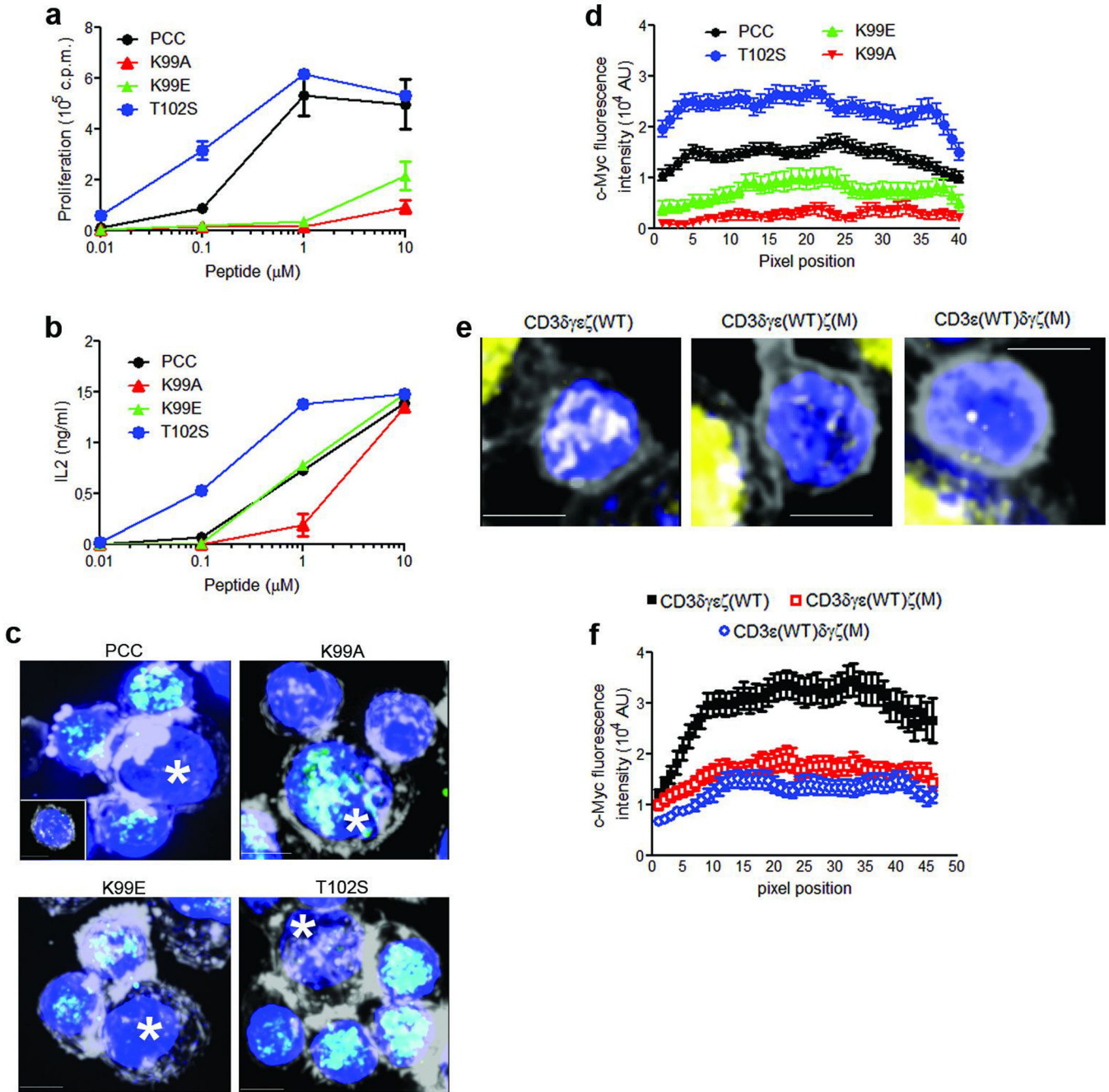
representative of three experiments, with 5 – 10 cells per group. HEK293 data are combined from 3–5 experiments. Statistical analyses were performed using one way ANOVA. Scale bars represent 5μm. Pixel size of STORM micrographs represent 30nm. * $p < 0.05$, ** $p < 0.001$, *** $p < 0.0001$.

Figure 7. Stimulation with weak agonists results in defective c-Myc induction
(**a,b**) Proliferative (**a**) and cytokine (**b**) responses were measured in response to stimulation of AND TCR transgenic T cells with control, weak agonist and super agonist peptides. Data are representative of 3 independent experiments with 6–10 mice per group. (**c,d**) Confocal microscopic analyses of c-Myc induction following stimulation with peptide-pulsed APC. Expression of nuclear c-Myc is presented as a line intensity statistic derived from a slice through the nucleus. Fluorescence intensity at each pixel is presented, with 50 cells per condition. (**e,f**) Retrogenic T cells expressing the AND TCR and wild-type or ITAM-mutant complexes were stimulated by PCC peptide-pulsed APC, followed by analysis of c-Myc.

Representative images are shown in (**e**) while fluorescence intensity is depicted in panel (**f**). Quantification data are representative of 3 independent experiments, while maximum projection images are depicted. APC are denoted with an asterisk where appropriate, and DAPI (blue), F-actin (grey) and c-Myc (green) are shown. Scale bars represent 5μm.